



Friction stir welding of thermoplastics with a new heat-assisted tool design: mechanical properties and microstructure

Ali Moochani¹ · Hamid Omidvar¹ · Seyed Reza Ghaffarian² · Seyed Mohammad Goushegir³

Received: 31 January 2018 / Accepted: 20 November 2018 / Published online: 7 December 2018
© International Institute of Welding 2018

Abstract

Traditional tools in friction stir welding (FSW) of thermoplastics fail to achieve high quality and strong welds. In this paper, a new heat-assisted stationary shoulder FSW tool design, which provides constant tool temperature during the process using a controllable hot air gun, is introduced. Effect of the process parameters, including tool temperature, rotational speed, and traverse speed, on the microstructure and mechanical properties of polypropylene sheets was investigated using Taguchi method and analysis of variance. Welded joints showed tensile strength up to 96% and elongation at break up to 99% of the base material. Samples with high mechanical performance showed a wider stir zone within thin flow layers, which arranged in a regular pattern, under polarized microscopy. Differential scanning calorimetry demonstrated that higher tool temperature results in lower degree of crystallinity. Scanning electron microscopy revealed that the sample with high mechanical properties has a craze-free fracture surface. However, the sample with the lowest mechanical properties produced a corrugated fracture surface full of crazes.

Keywords FSW · Auxiliary heating · Polypropylene · Entanglement · Mechanical properties · Microstructure

Abbreviations

PP	Polypropylene
FSW	Friction stir welding
HDPE	High-density polyethylene
ABS	Acrylonitrile butadiene styrene
RPM	Rotation per minute
DoE	Design of experiment
ANOVA	Analysis of variance

DSC	Differential scanning calorimetry
SEM	Scanning electron microscope

Recommended for publication by Commission XVI - Polymer Joining and Adhesive Technology

✉ Hamid Omidvar
omidvar@aut.ac.ir

¹ Department of Mining and Metallurgical Engineering, Amirkabir University of Technology (Tehran Polytechnic), Tehran 15875-4413, Iran

² Department of Polymer and Color Engineering, Amirkabir University of Technology (Tehran Polytechnic), Tehran 15875-4413, Iran

³ Helmholtz-Zentrum Geesthacht, Centre for Materials and Coastal Research, Institute of Materials Research, Materials Mechanics, Solid State Joining Processes, Max-Planck-Str. 1, 21502 Geesthacht, Germany

1 Introduction

Friction stir welding (FSW) is an advanced solid-state joining process, which was introduced in 1991 by The Welding Institute (TWI) of UK, initially applied to aluminum alloys [1]. The heating is achieved by friction between the tool and the workpiece as well as the plastic deformation of the welded materials [2].

The advantages of the FSW process over conventional fusion welding methods and the increasing demand for light-weight structures in industry have motivated the research in this field. In the case of FSW of thermoplastic materials, which is not an entire solid-state process [3], the technique is still unexploited comparing with metallic materials [4]. However, several research works have been done with the aim of evaluating the possibility of joining polymers with FSW.

It is claimed that obtaining good surface quality and high mechanical properties of the welded polymeric parts with conventional FSW tools is rather difficult [5]. Bozkurt [6] used a conventional tool for FSW of high-density polyethylene

Table 1 Selected physical and mechanical properties of polypropylene

Material	Tensile strength [MPa]	Elongation [%]	Density [g/cm ³]	Melting temperature [°C]
Polypropylene	27	570	0.9	155–165

(HDPE) sheets. The maximum tensile joint efficiency (the strength of the weld over the base material) was approximately 86.2%. Nelson et al. [7] developed a modified tool with a stationary shoulder, called a shoe, that is heated by electric resistance. In this technique, the shoe is responsible for providing a constraining surface to hold the material in the weld region during the welding process. Moreover, it introduces auxiliary heat in addition to the frictional energy produced by the tool. Several studies based on this technique were carried out using different polymers to optimize and evaluate the effects of this method on the weld seam properties. Among others, Azarsa et al. [8] investigated the flexural behavior of HDPE welds produced with a hot shoe. The optimum welding parameters were tool rotational speed of 1400 rpm, the tool traverse speed of 25 mm/min and shoulder temperature of 100 °C. The authors reported that the maximum flexural strength of the welded sample was about 96% of the base material strength. Bagheri et al. [9] used a similar method to weld acrylonitrile butadiene styrene (ABS) sheets and investigated the mechanical properties of welded joints. It was concluded that welding at high rotational speed and shoe temperature and a lower tool travel speed increases the weld quality and tensile strength.

An alternative tool design, known as the “self-reacting,” was developed by Pirizadeh et al. [10] to eliminate the root defect that is common in FSW of polymers. In this design, there are two stationary shoulders on both sides of the plate, which enable the process to reach complete penetration. Recently, new tool designs were developed, aiming at providing additional heat directly into the tool to eliminate the non-uniform heating exists in FSW. Vijendra and Sharma [11] used an induction heating system, which encloses the tool. They claimed that FSW of HDPE sheets with this tool ensures welds

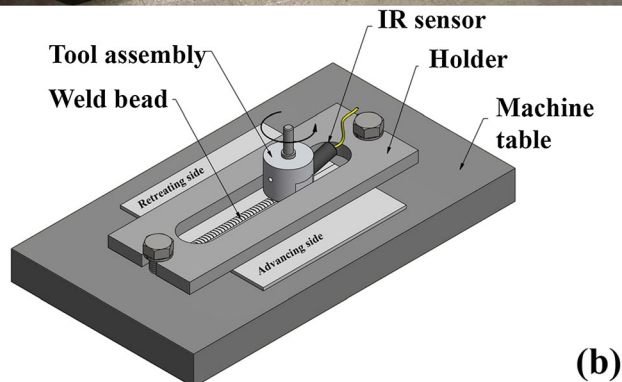


Fig. 2 Welding assembly during the process (a) and schematic representation of the setup (b)

with a similar strength to the base material, better than previously reported results. Although the tensile strength of the welds was comparable with the base material, the elongation of the welds was much lower than the base material. In a recent study, Banjare et al. [12] used an electrical resistance heater inside the rotating tool as the auxiliary heating system for FSW of polypropylene sheets. The highest tensile strength obtained was 14.57 MPa (55.5% of the base material) using a rotational speed of 720 rpm and additional heating. However, the highest elongation obtained (approximately 15%) was far from the elongation of the base material.

The main purpose of the present study was developing a new FSW tool, which could be capable of producing welds with mechanical properties similar or comparable to the base polymer. Polypropylene sheets were used as the base material.

Fig. 1 a FSW tool design. (b) Controllable hot air gun

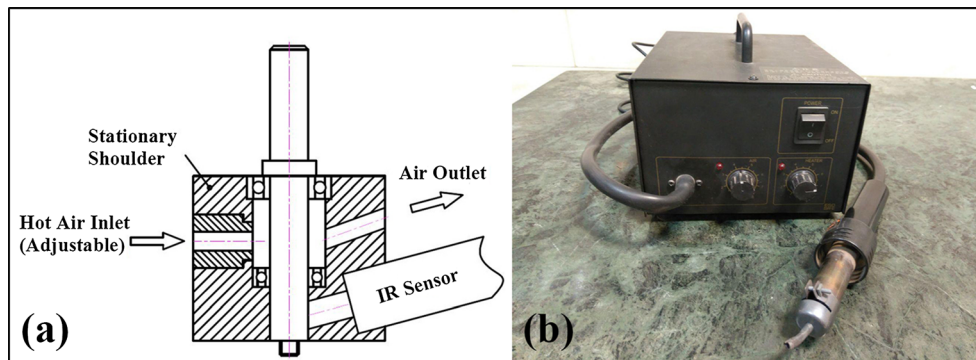
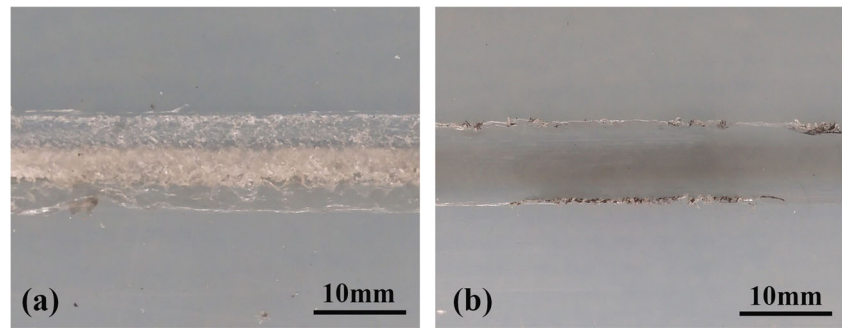


Fig. 3 PP sheets after friction stir welding. **a** None-heated. **b** Heat-assisted



Design of experiments (DoE) and statistical analysis using Taguchi method were used to evaluate the contribution of each welding parameter to the tensile strength and elongation of the welds. As a result of the unique design of this tool, it was possible to investigate the tool temperature as an independent process parameter in addition to the other parameters (i.e., rotational speed and traverse speed). Analysis of the FSW joints was performed by mechanical testing (tensile test), differential scanning calorimetry (DSC), polarized optical microscopy, and scanning electron microscopy (SEM).

2 Materials and methods

2.1 Material

In this study, Polypropylene (PP) sheets with the nominal thickness of 4 mm, supplied by Hyosung Korea were used as the base material. Polypropylene is a semicrystalline polymer with desirable physical, mechanical, and thermal properties when employed in room-temperature applications. It is relatively stiff and has a relatively high melting point, low density, and fairly good resistance to impact [13]. It also possesses excellent chemical resistance and low cost that make it the polymer of choice for various applications [13]. A summary of physical and mechanical properties of this polymer is listed in Table 1.

Tensile strength and elongation were obtained experimentally.

Density and melting temperature data were obtained from [14].

Table 2 Welding parameters and their respective levels

Welding parameter	Unit	Level 1	Level 2	Level 3
Tool temperature	°C	130	150	170
Rotational speed	rpm	950	565	360
Traverse speed	mm/min	24	40	60

2.2 Tool design

To compensate the lack of heat during FSW because of the low thermal conductivity and friction coefficient of polymers [15], applying an external heating source is advantageous to the weld quality. Moreover, it was proved that using stationary shoulder prevents the material ejection from the weld seam and improves the weld surface appearance [16]. In this work, a compact tool assembly with the stationary shoulder and the auxiliary heating source was developed. As illustrated in Fig. 1, the tool assembly consists of a stationary shoulder that encloses the FSW rotating tool. An infrared (IR) temperature sensor, a variable temperature heat gun, and two deep groove ball bearings are mounted on the shoulder. The advantage of this design over the others is the possibility of maintaining the pin temperature constant without changing the other parameters, i.e., rotational and traverse speed. For this purpose, the IR sensor monitors the pin temperature, and the variable temperature heat gun compensates for the intended pin temperature.

2.3 Experimental procedure

The polypropylene sheets were welded in a butt-joint configuration. The welding trials were performed on a universal milling machine with appropriate clamping fixtures and

Table 3 Experimental design using an L_9 orthogonal array

Welding condition	Welding parameters		
	Rotational speed [rpm]	Tool temperature [°C]	Traverse speed [mm/min]
1	950	130	24
2	950	150	40
3	950	170	60
4	565	150	24
5	565	170	40
6	565	130	60
7	360	170	24
8	360	130	40
9	360	150	60

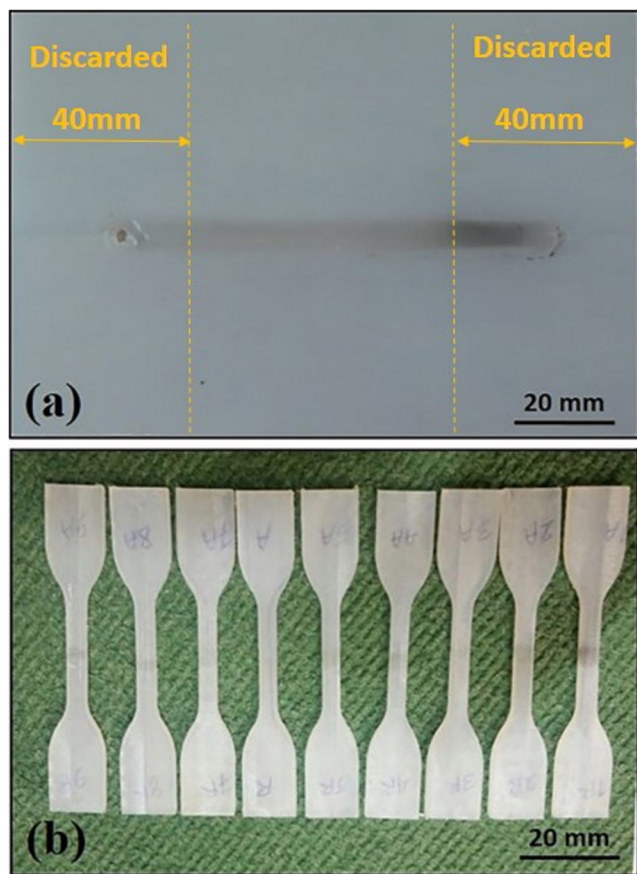


Fig. 4 a Extraction location of specimens in the welded joint. b Tensile specimens

mechanical settings. Figure 2 illustrates the welding assembly in this work. In the advancing side of the tool, which is indicated in Fig. 2b, the direction of the tool rotation and the direction of the tool traverse are the same, whereas in the retreating side, the tool rotation is in the opposite direction to the tool traverse.

A series of preliminary experiments was performed to select the relevant levels for each welding parameter, and the acceptance criterion for these levels was the appearance of the welds. It was observed that higher levels of the welding parameters than current levels results in the polymer ejection from the weld nugget. On the other hand, lower levels result in un-melted chip formation and rough surface. Figure 3 represents a comparison between none-heated (Fig. 3a) and heat-assisted (Fig. 3b) joints, both welded with 950 rpm rotational speed and 24 mm/min traverse speed. In addition to a better roughness of the weld surface, the heat-assisted joint showed higher strength than the none-heated weld, which could be separated even manually.

Classical experimental design methods are too complex and not easy to use. A large number of experiments have to be carried out when the number of the welding parameters increases [17]. Therefore, a DoE based on the Taguchi L9 orthogonal array was selected to perform the experiments, and the results of the mechanical testing were analyzed by the analysis of variance (ANOVA). Three levels for each welding parameter (i.e., rotation speed, traverse speed, and pin temperature) were chosen as listed in Tables 2 and 3. Tensile strength and elongation of the welds were selected as the main responses in the statistical analysis. As the higher level of mechanical properties are desirable in welded joints [17], the criterion “the-larger-the-better” for the S/N (signal to noise) ratio was chosen to figure out the optimal process parameters.

After welding, specimens were cut into tensile samples by the water-jet cutting process, in order to prevent morphological changes. As it is shown in Fig. 4, no specimens were taken from the first or last 40 mm of the welded sheets to remove the effects of the starting and finishing the FSW process. Tensile testing was performed in accordance with ASTM D638 standard at room temperature with a cross-head speed of 50 mm/

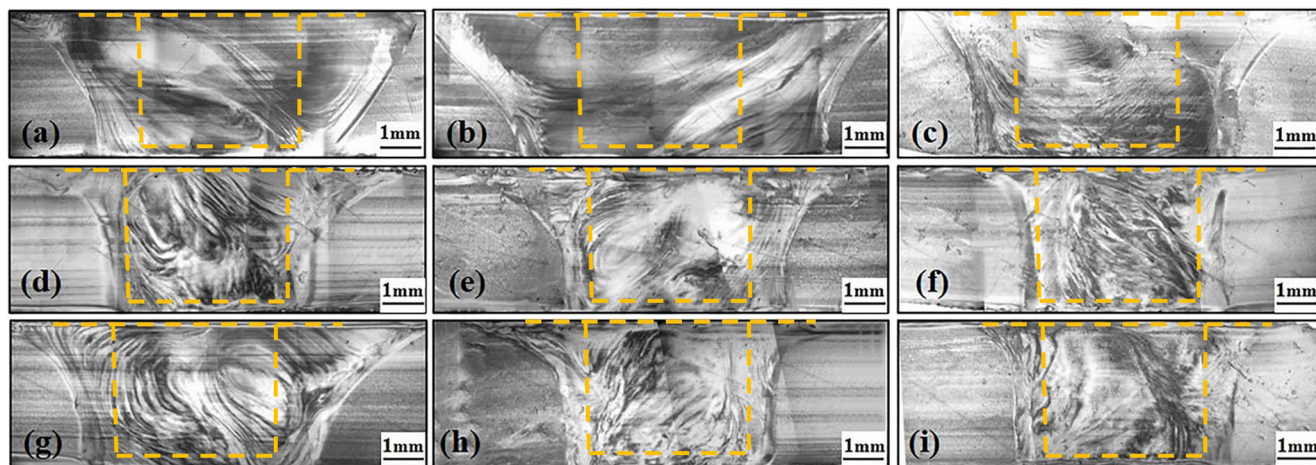


Fig. 5 Polarized micrographs of the weld cross sections. a–i Conditions 1 to 9, respectively (dash lines indicates the tool location during welding)

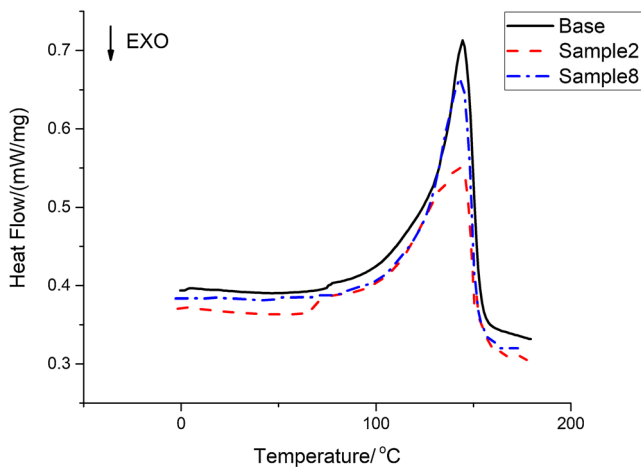


Fig. 6 DSC curves of PP welds under different conditions

min. Three replicates from each welding condition were tested to calculate the average tensile strength and elongation at break.

The morphology of weld seams was investigated using crossed polarized optical microscopy in transmission mode using an Olympus BX 51 (Tokyo, Japan) optical microscope. For this purpose, approximately 30- μm -thick slices were cut from the cross-sectional area of the welded specimens using a Leica RM 2235 microtome. The same slices used in polarized microscopy were analyzed for the comparison of crystallinity by differential scanning calorimetry (DSC) using a Mettler Toledo instrument. After tensile testing, fracture surface of some specimens was studied by SEM (JEOL JSM-6380LA, Tokyo, Japan).

3 Results and discussion

After successful runs for each combination of parameters according to Taguchi L9 orthogonal array, the results for output parameters, including tensile strength and elongation at break, have been extracted from the tensile testing results.

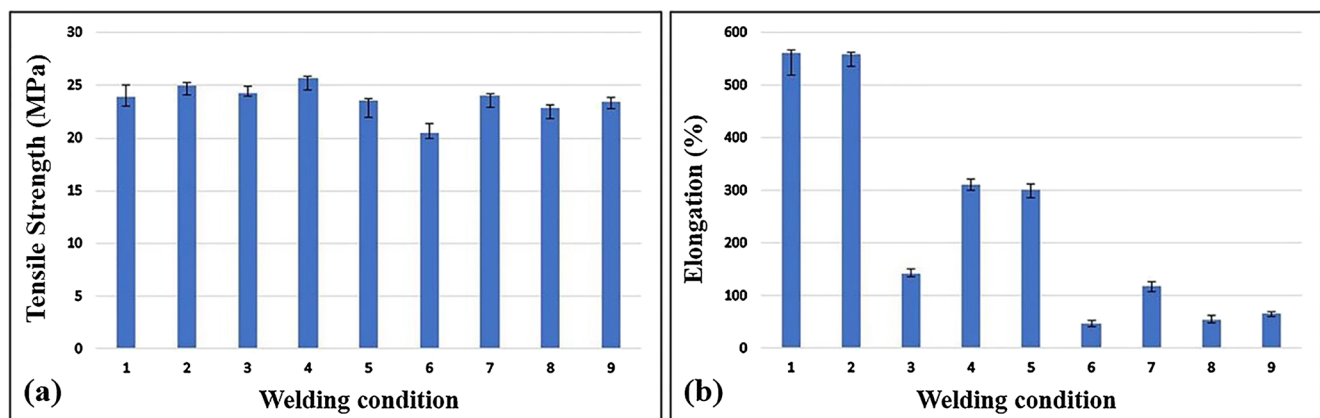


Fig. 7 a Tensile strength of the welds using different conditions. b Elongation

3.1 Microstructure of the welds

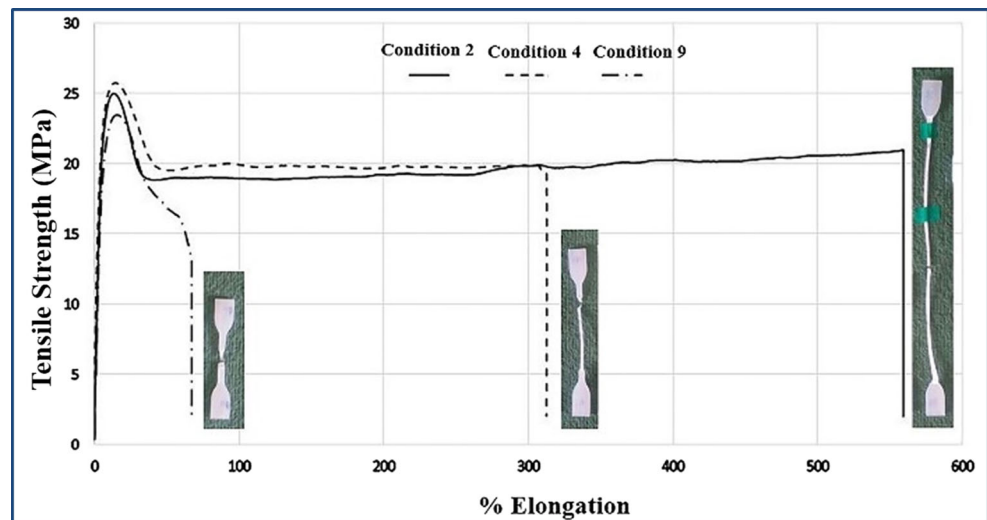
Figure 5 shows the polarized micrographs of the weld cross sections for all the samples.

A significant difference between the weld region (the stir zone or weld nugget) and the base material can be observed. The weld region in all samples shows a lamellar pattern of flow lines, as a result of the material mixing. These flow layers demonstrate the layers of material with similar molecular structure and orientation [18], as a consequence of material flow around the tool. Condition 2 (Fig. 5b), welded with a high rotational speed and medium tool temperature, showed a wide stir zone with the flow layers apparently closer and more uniform than other specimens. However, specimen 6 (Fig. 5f), welded with the highest traverse speed and lowest tool temperature, demonstrated a narrow stir zone with inhomogeneous flow layers. Welding with low heat input, such as condition 6, leads to a decreased amount of molten polymer with high viscosity, resulting in irregular flow layers and narrow stir zone. On the other hand, high rotational speed with low traverse speed produced thinner flow layers (in condition 2), which can be melted easily. This resulted in uniform flow layers with wider stir zone.

Conditions 1 and 2 (Fig. 5a, b) show the largest weld zone with a homogeneous pattern of flow layers. In these conditions, the temperature was high enough to plasticize the material. Moreover, the high rotational speed of the tool combined with lower tool traverse speed facilitates the material mixing. However, increasing the tool temperature to 170 °C (condition 3) tends to reduce the viscosity of the PP around the tool. High heat input as a result of high temperature and rotational speed reduces the material mixing particularly because of the high traverse speed of 60 mm/min. A slightly smaller welding zone (Fig. 5c) compared to conditions 1 and 2 with less clear flow lines are the result of the high heat input and traverse speed.

From conditions 4 to 6 (Fig. 5d–f), one observes that condition 6 has the smallest welding zone with very inhomogeneous

Fig. 8 Representative stress-strain curves from three welding conditions with low, medium, and large elongation



flow layers concentrated in the middle of the nugget. This is believed to be caused by the combination of the low heat input (lowest tool temperature) and very rapid traverse speed (60 mm/min). Besides that the heat generation might not be enough, the material does not have sufficient time to retain the temperature due to the high tool velocity. Furthermore, the rotational speed of 565 rpm was not enough to pull sufficient material from the retreating side to the advancing side and mix the material around the tool completely. In contrast, conditions 4 and 5 show a slightly larger weld nugget, where the material mixing and flow lines are distributed more homogeneously. Especially in condition 4, the lowest traverse speed gives more time to the material around the tool to be pulled from the retreating side and to be mixed.

Finally, one observes that condition 7 (Fig. 5g) also demonstrates a relatively large welding zone due to the high heat input (high tool temperature and low traverse speed). However, the flow layers are more concentrated in the retreating side (left side of the Figure). This means the mixing of the material was not very efficient as compared to conditions 1 and 2 because of the low rotational speed of 360 rpm. Conditions 8 and 9 show relatively small welding nugget with almost no flow layers visible. This is perhaps due to the low heat input as well as low rotational speed. Although both sheets were welded together strongly, the lack of material mixing is evident from Fig. 5h, i.

Table 4 Signal to noise ratios for elongation (the-larger-the-better)

Level	Tool temperature	Rotational speed	Traverse speed
1	40.94	50.90	48.67
2	46.99	44.25	46.35
3	44.68	37.46	37.59
Delta	13.45	13.45	11.08
Rank	3	1	2

3.2 Degree of crystallinity of the welds

The degree of crystallinity in polymers is highly affected by the thermal history experienced during manufacturing processes. A qualitative comparison of crystallinity between two samples (i.e., condition 2 and 8), welded with two different tool temperatures, has been conducted using DSC analyses. The results are shown in Fig. 6.

It can be demonstrated by the use of DSC curves (Fig. 6) that samples welded with higher tool temperatures poses a lower degree of crystallinity. As Nieh and Lee [19] stated in their work, the peak temperature of PP welds had a strong influence on the crystallization kinetics so that higher melt temperature could postpone the crystallization. Therefore, higher tool temperature in condition 2 has resulted in lower degree of crystallinity comparing to condition 8 and the base material. It could be concluded that as the tool temperature rises, the maximum temperature of the weld zone is increased. In other words, the tool temperature can represent the weld zone temperature.

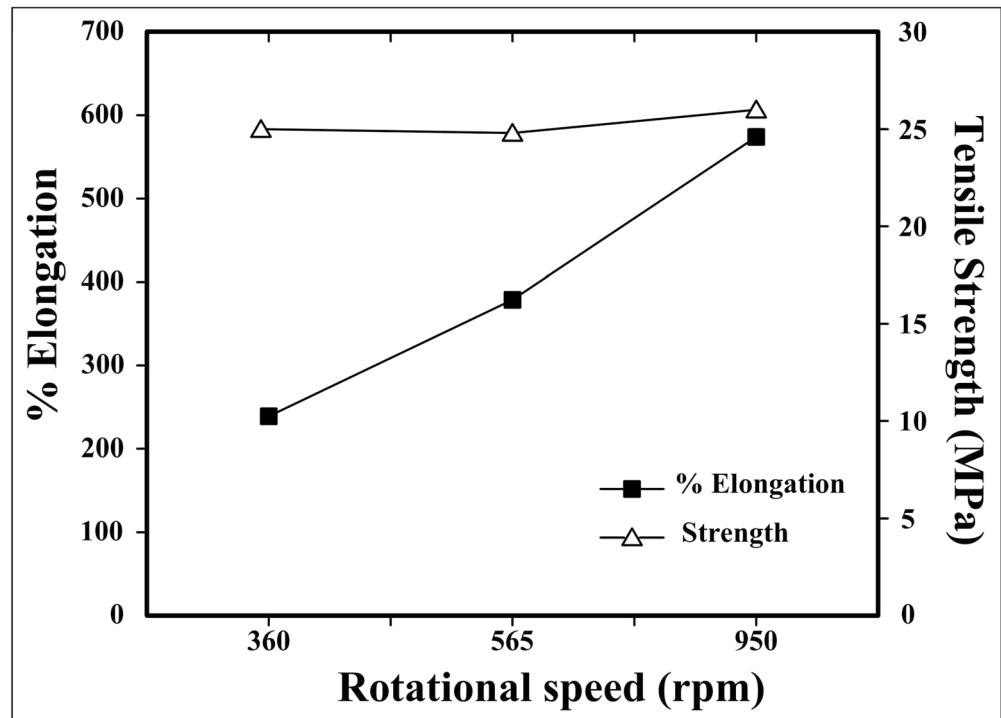
3.3 Mechanical properties of the welds

Figure 7 shows the average tensile strength and elongation of the welded specimens using different conditions. As can be

Table 5 Signal to noise ratios for strength (the-larger-the-better)

Level	Tool temperature	Rotational speed	Traverse speed
1	26.86	27.62	27.7
2	27.79	27.17	27.40
3	27.54	27.39	27.09
Delta	0.94	0.46	0.62
Rank	1	3	2

Fig. 9 Effect of the rotational speed on mechanical properties of the weld



seen in Fig. 7, the strength of the joints did not change significantly by changing the process parameters. However, the process parameters had a large influence on the elongation of the samples in the selected range. The tensile strength of the welds varied between 20 and 26 MPa (74 to 96% of the base material strength) and the elongation range was from 48 to 563% (8 to 99% of the base material elongation).

Figure 8 also shows a comparison between the stress-strain curves of the welded samples with a small, medium, and large elongation.

To investigate the statistical significance of each control parameter, the results obtained were analyzed in Minitab software under the condition “the-larger-the-better” in a Taguchi DoE. Orthogonal array design of Taguchi experiments allows

analyzing the individual effect of each process parameter on joint strength [20]. Tables 4 and 5 give the ANOVA results and the S/N ratios of the tensile strength and elongation. Delta in these tables indicates the maximum difference between the mean S/N ratio values in the three tested levels. Moreover, Figs. 9, 10, and 11 illustrate the influence of each process parameter on the mechanical properties of the welded specimens.

According to Tables 4 and 5, pin temperature is the most important process parameter changing the tensile strength, followed by traverse speed and tool rotational speed. In case of the elongation, tool rotational speed has the highest rank, followed by traverse speed and pin temperature.

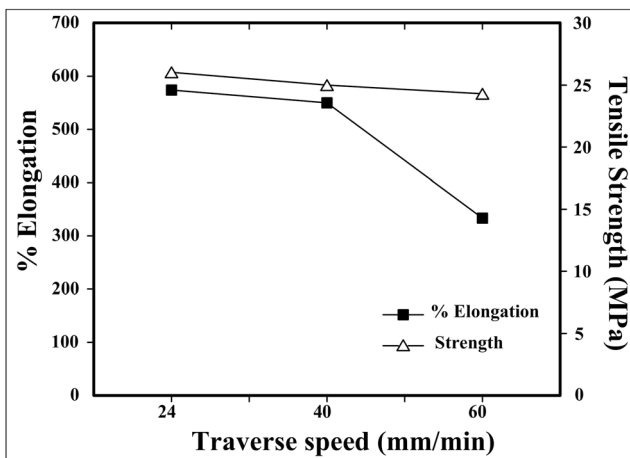


Fig. 10 Effect of the traverse speed on mechanical properties of the weld

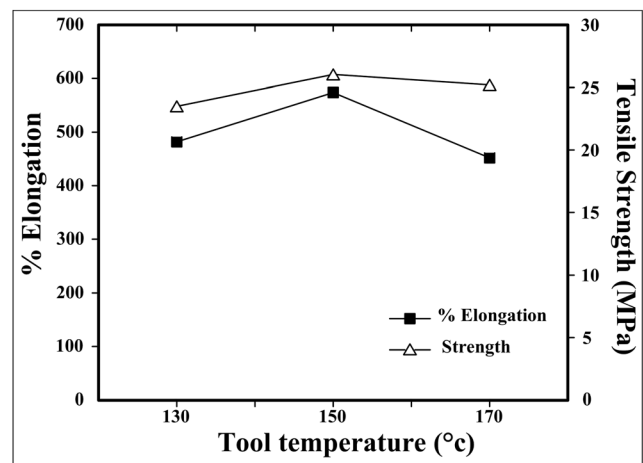


Fig. 11 Effect of the tool temperature on mechanical properties of the weld

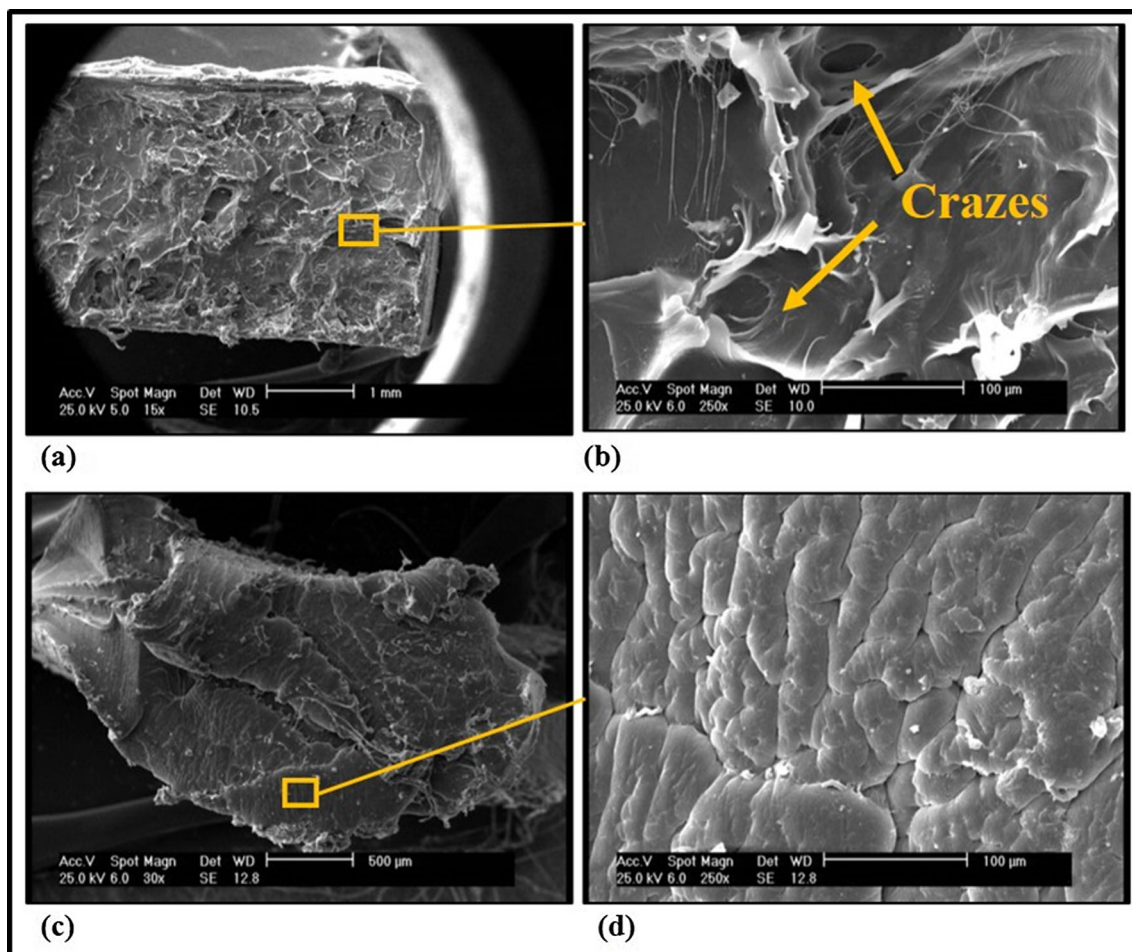


Fig. 12 SEM images of the fracture surfaces. **a, b** Specimen with lowest mechanical properties. **c, d** Specimen with highest mechanical properties

Condition 2 shows high mechanical properties (both strength and elongation) perhaps due to the high heat input. An important issue that should be noted here is the use of an innovative auxiliary heating source, which gives the assisting heat to the tool and keeps it at a constant temperature. Therefore, tool temperature parameter could represent the total amount of heat, supplied by frictional movement and auxiliary heating system.

As can be seen in Fig. 9, an increase in rotational speed results in a slight improvement in the strength and particularly a significant increase in the elongation of the welds. As explained earlier, higher rotational speed leads to a better material mixing by pulling more material from retreating side to the advancing side. Moreover, a better entanglement of the molecular chains within the welded zone may be achieved resulting in larger elongation and stronger welds. Medium and lower rotational speed leads to lower elongation because of the lower material mixing in the weld nugget as can also be observed from the micrographs in Fig. 5.

According to Fig. 10, increasing traverse speed decreases the mechanical properties of the welds. In particular, an increase in the traverse speed from 40 to 60 mm/min resulted in

a huge reduction in elongation of the welds. At higher travel speed, the polymer does not have enough time to flow, and insufficient material mixing happens, as was also reported by Husian et al. [21] and Payganeh et al. [22] in FSW of polyamide and polypropylene, respectively.

The other process parameter influencing the mechanical properties of the welds is the tool temperature. As can be seen in Fig. 11 an increase in the tool temperature up to 150 °C can improve both the strength and elongation of the weld. It is clear that higher tool temperature and consequently higher heat input increases the ability of the polymer to flow, leading to a better material mixing and a better entanglement of the molecular chains. However, excessive heat input (in this case tool temperature of 170 °C) may lead to a decrease in the degree of crystallinity and consequently mechanical properties.

3.4 Fracture surface of the welded joints

SEM was used to reveal the fracture surface of the welds and to obtain information about the processes of crack initiation and crack propagation. Figure 12 shows the SEM images of

the fracture surface from the failed specimens with highest and lowest mechanical properties (i.e., conditions 2 and 6). Figure 12a, b, at two different magnifications, shows the fracture surface of the sample welded in condition 6 which experienced the lowest elongation at break in tensile test. In contrast, Fig. 12c, d are related to the fracture surface of the sample welded in condition 2 which exhibited the highest elongation.

Comparing the fracture surfaces, one observes that condition 6 (Fig. 12a, b) produced a more corrugated appearance. Insufficient heat input and material mixing in this condition resulted in a poor entanglement between flow layers and as a result brittle fracture, which manifests itself in multiple crazing on fracture surface [23]. In contrast, condition 2 (Fig. 12a, b), which was welded with higher heat input and rotational speed, showed a ductile behavior and consequently nearly craze-free fracture surface [23].

4 Conclusions

In this study, a new friction stir welding tool with auxiliary heating source and stationary shoulder was introduced for joining polypropylene sheets. The effects of friction stir welding parameters on the mechanical properties of the welds were evaluated using the Taguchi design of experiments and the analysis of variance. Cross-sectional area and fracture surface of the welds were also investigated by polarized light microscopy and scanning electron microscopy. Moreover, the degree of crystallinity was investigated using differential scanning calorimetry. The following key conclusions were obtained:

- Using the tool design with auxiliary heating enabled friction stir welding of polypropylene sheets with constant tool temperature.
- Welds with mechanical properties comparable to those of the polypropylene base material were obtained.
- Welds with higher mechanical properties showed more uniform flow layers, which were apparently also closer to each other than the welds with lower mechanical properties.
- Welds with the tensile strength up to 96% and the elongation up to 98% of the base material properties were achieved.
- DSC analyses revealed that the samples welded with higher tool temperatures had lower degree of crystallinity.
- The most dominant welding parameter affecting the tensile strength was the tool temperature and that for the elongation was the rotational speed.
- The effect of welding parameters on the elongation of the welds was apparently larger than on the tensile strength of the specimens.

- SEM investigation reveals that the sample with the lowest elongation (condition 6) produced a corrugated fracture surface accompanied by crazes, which may be a result of poor entanglement and material mixing within the welding zone.
- The fracture surface of the sample with the highest elongation (condition 2) showed no signs of crazes.

References

1. Thomas WM, Nicholas ED, Needham JC, Murch MG, Templesmith P, Dawes CJ (1995) Friction welding (U.S. Patent 5,460,317)
2. Thomas WM, Staines DG, Norris IM, de Frias R (2003) Friction stir welding tools and developments. *Weld World* 47(11–12):10–17. <https://doi.org/10.1007/BF03266403>
3. Derazkola HA, Kashiry Fard R, Khodabakhshi F (2018) Effects of processing parameters on the characteristics of dissimilar friction-stir-welded joints between AA5058 aluminum alloy and PMMA polymer. *Weld World* 62(1):117–130. <https://doi.org/10.1007/s40194-017-0517-y>
4. Paoletti A, Lambiasi F, Di Ilio A (2016) Analysis of forces and temperatures in friction spot stir welding of thermoplastic polymers. *Int J Adv Manuf Technol* 83(5–8):1395–1407. <https://doi.org/10.1007/s00170-015-7669-y>
5. Eslami S, Tavares PJ, Moreira P (2016) Friction stir welding tooling for polymers: review and prospects. *Int J Adv Manuf Technol* 50:1. <https://doi.org/10.1007/s00170-016-9205-0>
6. Bozkurt Y (2012) The optimization of friction stir welding process parameters to achieve maximum tensile strength in polyethylene sheets. *Mat Des* 35:440–445. <https://doi.org/10.1016/j.matdes.2011.09.008>
7. Nelson TW, Sorenson CD, Johns CJ (2004) Friction stir welding of polymeric materials (U.S. Patent NO. 6,811,632)
8. Azarsa E, Mostafapour A (2014) Experimental investigation on flexural behavior of friction stir welded high density polyethylene sheets. *J Manuf Process* 16(1):149–155. <https://doi.org/10.1016/j.jmapro.2013.12.003>
9. Bagheri A, Azdast T, Doniavi A (2013) An experimental study on mechanical properties of friction stir welded ABS sheets. *Mat Des* 43:402–409. <https://doi.org/10.1016/j.matdes.2012.06.059>
10. Pirzadeh M, Azdast T, Rash Ahmadi S, Mamaghani Shishavan S, Bagheri A (2014) Friction stir welding of thermoplastics using a newly designed tool. *Mat Des* 54:342–347. <https://doi.org/10.1016/j.matdes.2013.08.053>
11. Vijendra B, Sharma A (2015) Induction heated tool assisted friction-stir welding (i-FSW): a novel hybrid process for joining of thermoplastics. *J Manuf Process* 20:234–244. <https://doi.org/10.1016/j.jmapro.2015.07.005>
12. Banjare PN, Sahlot P, Arora A (2017) An assisted heating tool design for FSW of thermoplastics. *J Mater Process Technol* 239: 83–91. <https://doi.org/10.1016/j.jmatprotec.2016.07.035>
13. Kissel WJ, Han JH, Meyer JA (2003) Polypropylene: structure, properties, manufacturing processes, and applications. In: Karian HG (ed) *Handbook of polypropylene and polypropylene composites*. Marcel Dekker Inc., New York, pp 10–27
14. Yan B, Wu H, Jiang G, Guo S, Huang J (2010) Interfacial crystalline structures in injection over-molded polypropylene and bond strength. *ACS Appl Mater Interfaces* 2(11):3023–3036. <https://doi.org/10.1021/am1003574>

15. Aydin M (2010) Effects of welding parameters and pre-heating on the friction stir welding of UHMW-polyethylene. *Poly Plast Technol Eng* 49(6):595–601. <https://doi.org/10.1080/03602551003664503>
16. Kiss Z (2011) Microscopic analysis of the morphology of seams in friction stir welded polypropylene. *Express Polym Lett* 6(1):54–62. <https://doi.org/10.3144/expresspolymlett.2012.6>
17. Bilici MK (2012) Application of Taguchi approach to optimize friction stir spot welding parameters of polypropylene. *Mat Des* 35:113–119. <https://doi.org/10.1016/j.matdes.2011.08.033>
18. Seth R, Strand (2004) Effects of friction stir welding on polymer microstructure
19. Nieh J, James Lee L (1998) Hot plate welding of polypropylene. Part I: crystallization kinetics. *Polym Eng Sci* 38(7):1121–1132
20. Esteves JV, Goushegir SM, Dos Santos JF et al (2015) Friction spot joining of aluminum AA6181-T4 and carbon fiber-reinforced poly(phenylene sulfide): effects of process parameters on the microstructure and mechanical strength. *Mat Des* 66:437–445. <https://doi.org/10.1016/j.matdes.2014.06.070>
21. Husain IM, Salim RK, Azdast T et al (2015) Mechanical properties of friction-stir-welded polyamide sheets. *Int J Mech Mater Eng* 10(1):241. <https://doi.org/10.1186/s40712-015-0047-6>
22. Payganeh GH, Arab NM, Asl YD et al (2011) Effects of friction stir welding process parameters on appearance and strength of polypropylene composite welds. *Int J Phy Sci* 6(19):4595–4601. <https://doi.org/10.5897/IJPS11.866>
23. Hening S and Michler GH (2005) Micromechanical deformation mechanisms in polyolefins: influence of polymorphism and molecular weight. In: Michler GH and Baltá-Calleja FJ (eds) *Mechanical properties of polymers based on nanostructure and morphology*. Taylor & Francis, pp 245–278